

# Investigating the Mechanobiology of Cancer Cell–ECM Interaction Through Collagen-Based 3D Scaffolds

CHIARA LIVERANI,<sup>1,4</sup> LAURA MERCATALI,<sup>1</sup> LUCA CRISTOFOLINI,<sup>2,3</sup> EMANUELE GIORDANO,<sup>3,4,5</sup>  
SILVIA MINARDI,<sup>6</sup> GIOVANNA DELLA PORTA,<sup>7</sup> ALESSANDRO DE VITA,<sup>1</sup> GIACOMO MISEROCCHI,<sup>1</sup>  
CHIARA SPADAZZI,<sup>1</sup> ENNIO TASCIOTTI,<sup>6</sup> DINO AMADORI,<sup>1</sup> and TONI IBRAHIM<sup>1</sup>

<sup>1</sup>Osteoncology and Rare Tumors Center, Istituto Scientifico Romagnolo per lo Studio e la Cura dei Tumori (IRST) IRCCS, Via P. Maroncelli, 40, 47014 Meldola, Italy; <sup>2</sup>Department of Industrial Engineering (DIN), Alma Mater Studiorum – University of Bologna, Bologna, Italy; <sup>3</sup>BioEngLab, Health Science and Technology, Interdepartmental Center for Industrial Research (HST-CIRI), Alma Mater Studiorum – University of Bologna, Ozzano Emilia, Italy; <sup>4</sup>Laboratory of Cellular and Molecular Engineering “S.Cavalcanti”, Department of Electrical, Electronic and Information Engineering “G.Marconi” (DEI), Alma Mater Studiorum – University of Bologna, Cesena, Italy; <sup>5</sup>Advanced Research Center on Electronic Systems (ARCES), Alma Mater Studiorum – University of Bologna, Bologna, Italy; <sup>6</sup>Center for Biomimetic Medicine, Houston Methodist Research Institute, Houston, TX, USA; and <sup>7</sup>Translational Medicine Laboratory, Department of Medicine, Surgery and Dentistry, University of Salerno, Baronissi, Italy

(Received 22 September 2016; accepted 25 February 2017; published online 6 March 2017)

Associate Editor Chwee Teck Lim oversaw the review of this article.

**Abstract**—Deregulated dynamics of the extracellular matrix (ECM) are one of the hallmarks of cancer. Studies on tumor mechanobiology are thus expected to provide an insight into the disease pathogenesis as well as potentially useful biomarkers. Type I collagen is among the major determinants of breast ECM structural and tensile properties, and collagen modifications during tumor evolution drive a number of disease-related processes favoring cancer progression and invasion. We investigated the use of 3D collagen-based scaffolds to identify the modifications induced by cancer cells on the mechanical and structural properties of the matrix, comparing cell lines from two breast tumor subtypes with different clinical aggressiveness. Orthotopic implantation was used to investigate the collagen content and architecture of *in vivo* breast tumors generated by the two cell lines. MDA-MB-231, which belongs to the aggressive basal-like subtype, increased scaffold stiffness and overexpressed the matrix-modifying enzyme, lysyl oxidase (LOX), whereas luminal A MCF-7 cells did not significantly alter the mechanical characteristics of extracellular collagen. This replicates the behavior of *in vivo* tumors generated by MDA-MB-231, characterized by a higher collagen content and higher LOX levels than MCF-7. When LOX activity was blocked, the ability of MDA-MB-231 to alter scaffold stiffness was impaired. Our model could constitute a relevant *in vitro* tool to reproduce and investigate the biomechanical interplay subsisting between cancer cells and the surrounding ECM and its impact on tumor phenotype and behavior.

**Keywords**—Cancer biomechanics, Collagen scaffolds, Breast tumors, Stiffness, Aggressive cells.

Address correspondence to Chiara Liverani, Osteoncology and Rare Tumors Center, Istituto Scientifico Romagnolo per lo Studio e la Cura dei Tumori (IRST) IRCCS, Via P. Maroncelli, 40, 47014 Meldola, Italy. Electronic mail: chiara.liverani@irst.emr.it

## INTRODUCTION

The extracellular matrix (ECM) has a vital role in the regulation of various biological pathways contributing to development, tissue homeostasis and diseases.<sup>5</sup> ECM properties are modified in multiple pathological processes either as a cause or a result of the disease pathogenesis.<sup>5</sup> In cancer, it is known that ECM remodeling is capable of fostering a number of tumor processes such as progression<sup>24</sup> and metastasis initiation.<sup>33</sup> In particular, breast cancer has been defined as a disease of altered mechanobiology: matrix density, structure and stiffness, together with interstitial fluid pressure and flow, change during tumor evolution.<sup>13</sup> As an example, the collagen matrix of breast cancer stroma is significantly stiffer and more linearized than in normal tissue, due to a progressive enzymatic crosslinking mediated by cancer cells.<sup>24</sup> Linearized collagen fibers can substantially increase growth factor-dependent cell migration and directly promote tumor progression.<sup>24</sup> In addition, altered mechanical signaling affects cell survival, motility, division, and differentiation.<sup>12,15,21</sup> Investigations into these processes provided a new insight into breast cancer pathogenesis, leading to the identification of clinically useful biomarkers. It has been shown that an ECM gene signature can stratify breast cancer patients into subclasses that predict outcome.<sup>3</sup> Furthermore, increased breast tumor density in mammography has proven to be significantly correlated with reduced

progression-free survival in metastatic patients<sup>14</sup> and to be an excellent predictor of response to tamoxifen in the preventive setting.<sup>11</sup>

*In vitro* research offers several experimental methods and models to investigate the tumor mechanobiology.<sup>8</sup> In particular, tridimensional (3D) biomimetic matrices provide the ideal tools to efficiently recapitulate tissue dimensionality and the biomechanical and physical cues of tumor ECM.<sup>19</sup> A number of 3D systems have been used to investigate how cancer cells interact with the ECM, or to address the impact of mechanical signaling in diverse tumor phenotypes and behaviors.<sup>9,29,40</sup> Collagen is a major component of the breast connective tissue and is a key determinant of its tensile properties<sup>34</sup> and of the macroscopic deformability of mammary tumors<sup>16</sup> that are characterized by increased collagen content and remodeling.<sup>35</sup>

In the present study we used a porous type I collagen scaffold to investigate the ability of breast cancer cells to produce alteration in the material mechanical characteristic. This biomimetic matrix, providing a physiological network in 3D, constitutes the model of choice to reproduce *in vitro* the cell–ECM interactions. Specifically, we assessed the modifications induced by cancer cells on the compressive stiffness of the scaffolds, comparing cell lines of two breast tumor subtypes characterized by different clinical aggressiveness and distinct ECM characteristics. The aim was to demonstrate whether this 3D model might offer a valid and informative tool to recapitulate and investigate the

biomechanical interaction between cancer cells and the surrounding ECM.

## MATERIALS AND METHODS

### *In Vitro Experimental Model*

Two different human breast cancer cell lines, MCF-7 and MDA-MB-231, were cultured for 10 days on 3D porous collagen scaffolds. MCF-7 cells belong to the luminal A subtype of breast cancer and are associated with weak *in vitro* invasiveness, whereas MDA-MB-231 belong to the basal-like subtype and are associated with an invasive behavior<sup>17</sup> and the ability to colonize different sites (e.g. bone, liver, lung and brain) after intravenous injection.<sup>22</sup> At the end of the culture time, the phenotypes of the two cell lines were characterized by morphological and molecular analyses, while the mechanical and structural properties of the scaffolds were tested to assess the modifications induced in the collagen matrix by either cell line (Fig. 1a).

### *Synthesis of the Porous Collagen Scaffolds*

All chemicals were purchased from Sigma Aldrich (USA). The scaffolds were synthesized from type I bovine collagen, as described elsewhere.<sup>26</sup> Briefly, a 1 wt% collagen suspension in acetate buffer (pH 3.5) was prepared. The collagen was then precipitated to pH 5.5 with NaOH 1 M. The collagen was then

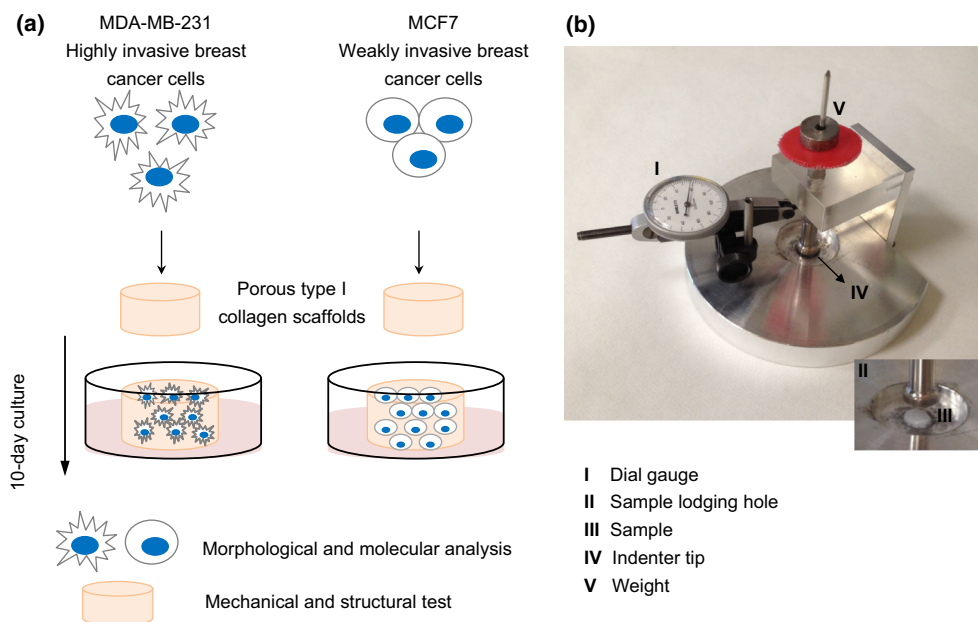


**FIGURE 1.** (a) Two human breast cancer cell lines, MCF-7 and MDA-MB-231, characterized by a diverse aggressive behavior, were cultured for 10 days on porous collagen-based 3D scaffolds. At the end of the culture time, cells were characterized for morphological and molecular phenotypes and the mechanical and structural properties of the scaffolds were analyzed; (b) photo of the prototype device used to measure the compressive modulus of the collagen scaffolds.

washed three times with deionized water and then crosslinked in an aqueous solution of 1,4-butanediol diglycidyl ether (BDDGE) (2.5 mM), for 24 h. Finally, the collagen was washed three times and casted in Teflon molds (9 mm in diameter) and freeze dried through an optimized freezing and heating ramp to obtain the desired pore size and porosity (from 25 to  $-25^{\circ}\text{C}$  and from  $-25$  to  $25^{\circ}\text{C}$  in 50 min,  $p = 0.20$  mbar). The morphology of the scaffold was characterized by scanning electron microscopy (SEM) and the pore size determined by ImageJ (US National Institutes of Health); the swelling properties of the scaffold and overall porosity were determined through water and ethanol infiltration methods.<sup>26</sup> Mean diameters were determined by caliper measurement. All analyses were performed on both control scaffolds and scaffolds after a 10-day culture with MCF-7 and MDA-MB-231 (after the decellularization step).

#### *Cell Seeding and Culture*

MCF-7 and MDA-MB-231 cell lines were obtained from the American Type Culture Collection (USA). All cells were maintained in DMEM medium supplemented with 10% fetal bovine serum, 1% penicillin–streptomycin and 1% glutamine (PAA, USA) at  $37^{\circ}\text{C}$  in a 5%  $\text{CO}_2$  atmosphere. Each scaffold was placed in a 6-multiwell plate and seeded with  $5 \times 10^{12}$  cells by dropping 50  $\mu\text{L}$  of the cell suspension on the scaffold. Cells were allowed to adhere for 1 h at  $37^{\circ}\text{C}$ , after which 4 mL of culture medium were gently added to each well. After a 24-h incubation, all scaffolds were carefully removed and placed in a new 6-multiwell plate. Medium was replaced daily. Uncellularized control scaffolds were maintained in cell-free culture medium at the same temperature and humidity conditions.

#### *Cell Quantification*

The number of cells infiltrating the scaffold on day 10 was assessed by total DNA content quantification using the PicoGreen dsDNA assay (Invitrogen, Carlsbad, CA, USA). The total DNA was extracted using DNeasy Blood & Tissue Kit (Qiagen, Duesseldorf, Germany) following the manufacturer's instructions and 100  $\mu\text{L}$  of DNA mixture were then added to 100  $\mu\text{L}$  of PicoGreen reagent working solution. Fluorescence of the samples was measured with a microplate reader (FLUOstar OPTIMA BMG LABTECH, Ortenberg, Germany), with excitation and emission wavelengths of 480 and 520 nm, respectively. The total number of cells was determined using the conversion factor of 7.7 pg DNA/cell.

#### *Histological Analysis*

The collagen constructs were fixed in 10% neutral buffered formaldehyde and dehydrated in a graded series of ethanol. Samples were then embedded in paraffin, sliced at a thickness of 5  $\mu\text{m}$  with a rotating microtome (Leica Biosystems, USA) and mounted on Superfrost Plus microslides (Thermo Fisher Scientific, USA). Hematoxylin and eosin (H&E) staining was performed to evaluate cell morphology and distribution in the scaffold matrix.

#### *LOX Inhibition*

The activity of LOX was blocked by the irreversible LOX inhibitor,  $\beta$ -aminopropionitrile (BAPN) (Sigma Aldrich).<sup>4,27,42</sup> MDA-MB-231 cells within the scaffold were treated with 500  $\mu\text{M}$  of BAPN 24 h after seeding. BAPN was administered on a daily basis until the end of the experiment. On day 10 the culture was stopped, cell proliferation with or without LOX inhibition was assessed by MTT assay, and the mechanical test was performed.

#### *Scaffold Decellularization*

The scaffolds were decellularized in 0.5% Triton X-100 for 1 h at room temperature and then washed three times in phosphate saline buffer (PBS). Uncellularized scaffolds were exposed to the same decellularization process to ensure that the experimental conditions did not contribute to scaffold mechanical properties. Decellularization was confirmed by the absence of MTT metabolization. The remaining DNA content of the decellularized scaffolds was assessed as follows: total DNA was extracted using the DNeasy Blood & Tissue Kit (Qiagen, Germany) following the manufacturer's instructions and quantified with a Nano-Drop ND-1000 spectrophotometer.

#### *Mechanical Testing*

We developed a prototype loading device to apply a state of unconfined uniaxial compression to the collagen scaffolds (Fig. 1b). This in-house built instrument consisted of a base support with a cylindrical hole (diameter 30 mm, depth 0.5 mm) designed to lodge the scaffold specimen, and a cylindrical piston (diameter 10 mm) to indent the specimen with known force values. The applied stress ( $\sigma$ , in kPa) could then be computed by dividing the applied force by the cross section of the specimen. The applied force consisted of a pre-load of 0.09 N (corresponding to a pre-stress of 1.41 kPa), which was held constant for 30 s; the full load of 0.38 Newton (corresponding to 5.97 kPa) was

then constantly applied for 30 s. Such holding times were sufficient for the visco-elastic time-dependent deformation to reach an equilibrium. The piston was equipped with a dial gauge (Borletti, Milan, Italy) to measure the piston displacement while the specimen was compressed. The consequent strain ( $\epsilon$ , dimensionless) was computed by dividing the measured piston displacement by the height of the specimen. The dial gauge had a resolution of 0.002 mm (corresponding to a resolution of 0.1% for the strain). The stiffness (compressive modulus, in kPa) of the collagen scaffold was computed as the ratio between the increment of stress and increment of strain from the pre-load to the full load values.<sup>2</sup> The specimens were tested in air immediately after having been removed from the PBS where they were soaked. The compressive modulus of collagen scaffolds decellularized after a 10-day culture with MCF-7 or MDA-MB-231 was compared with that of uncellularized scaffolds. Five specimens of each type were tested. Each specimen was tested 10 times to improve the quality of the measurement. The compressive modulus of each specimen was computed as the average of the 10 repeated measurements.

#### *Microscopy Analysis*

The collagen scaffolds were imaged by SEM and Laser Confocal Microscopy. For SEM imaging, samples were washed in 0.1 M sodium cacodylate buffer pH 7.4 and fixed in 2.5% glutaraldehyde in 0.1 M sodium cacodylate buffer pH 7.4 for 2 h at 4 °C. Samples were then dehydrated in a graded series of ethanol, desiccated and sputter-coated with platinum. Images were acquired with a Nova NanoSEM (FEI, USA). For confocal imaging, cells were washed in 1% PBS and fixed with 4% paraformaldehyde for 20 min at room temperature. Images were taken with an A1 laser confocal microscope (Nikon Corporation, Japan).

#### *Quantitative Real-Time Reverse Transcription-PCR (qRT-PCR)*

Total mRNA was isolated using TRIzol Reagent (Invitrogen, USA) following the manufacturer's instructions. Five hundred nanograms of RNA were reverse-transcribed using the iScript cDNA Synthesis Kit (BioRad, USA). The final mixture was incubated at 25 °C for 5 min, 42 °C for 20 min, 47 °C for 20 min, 50 °C for 15 min, and finally a 85 °C for 5 min. Real Time-PCR was performed in a 7500 Real-Time PCR System (Applied Biosystems, USA) using the TaqMan universal assay mix (Applied Biosystems). Amplification was performed in a final volume of 20  $\mu$ L con-

taining 2 $\times$  Gene Expression Master Mix (Applied Biosystems) and 2  $\mu$ L of cDNA. The reaction mixtures were all subjected to 2 min at 50 °C, 10 min at 95 °C followed by 40 PCR cycles at 95 °C for 15 s and 60 °C for 1 min. The stably expressed endogenous  $\beta$ -actin and HPRT were used as reference genes. Three target markers were analyzed: vimentin (VIM), E-cadherin (CDH1) and lysyl oxidase (LOX). The amount of these transcripts was normalized to the endogenous reference genes and expressed as n-fold mRNA levels relative to a calibrator using the comparative threshold cycle (Ct) value method ( $\Delta\Delta$ Ct). The calibrator used for all the analyses was a mix of the RNA extracted from MCF7 and MDA-MB-231 in standard monolayer cultures.

#### *MTT Assay*

Cell survival in MDA-MB-231 treated with the LOX inhibitor BAPN was assessed by MTT assay. Briefly, the scaffolds were incubated for 2 h at 37 °C in 0.5 mg/mL of MTT solution (Sigma Aldrich). After solubilization in acidic isopropanol, the absorbance was read at 550 nm. Cell survival was determined by comparing the average absorbance of cells in the absence or presence of BAPN treatment.

#### *Xenograft Study*

To establish orthotopic breast tumors, MCF-7-Luc2 and MDA-MB-231-Luc2 cells, both marked with a luciferase probe, were suspended in 100  $\mu$ L of matrigel (BD, Franklin Lakes, NJ, USA) at a concentration of  $5 \times 10^{12}$  cells and orthotopically injected into the right mammary fat pad of 8 week-old female immunodeficient nu/nu nude mice. Tumor growth was followed by *in vivo* bioluminescence imaging and caliper measurement every 2–3 days after the injection. After 4 weeks, tumors were resected and embedded in Optimal Cutting Temperature (OCT) compound and cryo-sectioned.

#### *Collagen Staining*

Trichrome staining and Picrosirius red were performed on the OCT-embedded frozen tissues to study the tumor collagen matrix, and on collagen scaffold sections. Trichrome staining (Abcam) was performed according to manufacturer's instructions. For Picrosirius red the frozen sections were stained with 0.1% (Direct Red 80) (Sigma Aldrich) sirius red in saturated aqueous solution of picric acid and counterstained with Weigert's hematoxylin. The RGB images were analyzed by ImageJ.

### Statistical Analysis

At least three independent experiments were performed. Data are presented as mean  $\pm$  standard error (SE), with *n* indicating the number of replicates. For *in vitro* and *in vivo* data, differences between groups were assessed by a two-tailed Student's *t* test and accepted as significant at  $p < 0.05$ .

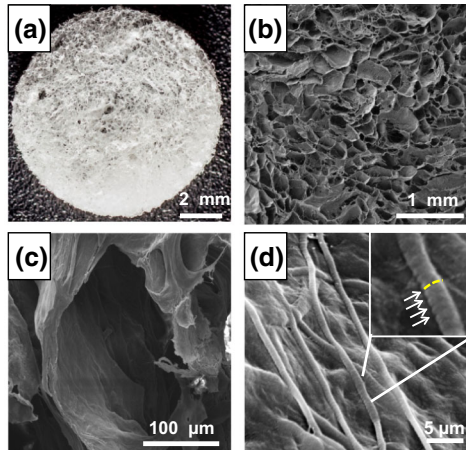
## RESULTS

### Collagen Scaffold Properties

The collagen scaffolds had a mean diameter of  $9 \pm 0.5$  mm (Fig. 2a) and a mean thickness of 2 mm. The size of the pores ranged from 150 to 300  $\mu\text{m}$ , with a mean pore size of  $197 \pm 25$   $\mu\text{m}$  (Fig. 2b and 2c). Collagen fibers showed a high degree of structural assembling and preserved their typical D-bands (arrowhead) (Fig. 2d) a characteristic axial D-periodic (67 nm) morphology derived from the self-assembly of single collagen molecules. The scaffolds displayed a mean porosity percentage of  $87.8 \pm 4.1$  (Fig. 2e).

### Collagen Remodeling in Breast Xenograft Tumors

Orthotopic implantation of MCF-7 and MDA-MB-231 in female immunodeficient mice was performed to



(e)

#### Collagen scaffold properties

Diameter:	$9 \pm 0.5$ mm
Pore diameter distribution:	150-300 $\mu\text{m}$
Average pore diameter:	$197 \pm 25$ $\mu\text{m}$
Porosity (%)	$87.8 \pm 4.1$

**FIGURE 2.** (a) Photos of the collagen-based scaffold; (b–d) SEM analysis of the scaffolds at different magnifications with the typical D-bands (d) identified by white arrows and a yellow dotted line showing their axial disposition; (e) scaffold macro- and micro-properties.

investigate the collagen content and architecture in the ECM of *in vivo* breast tumors. After 4 weeks both cell lines had developed detectable mammary tumors. Bioluminescence imaging and caliper measurement showed that MCF-7 grew considerably slower than MDA-MB-231 displaying a mean tumor volume of  $70 \pm 15$   $\mu\text{m}^3$  compared to  $388 \pm 68$   $\mu\text{m}^3$  of MDA-MB-231 (Fig. 3a). Trichrome staining of resected tumor sections revealed a higher presence of thick collagen fibers in MDA-MB-231 orthotopic tumors compared to those generated by MCF-7 (Fig. 3b). Moreover, quantification of the collagen percentage in Picosirius red stained sections showed that MDA-MB-231 tumors displayed a significantly higher collagen content than that of MCF-7 ones ( $p = 0.0005$ ) (Fig. 3c). Finally, the *in vivo* expression of the matrix crosslinking enzyme LOX was markedly higher for MDA-MB-231 than for MCF-7 (Fig. 3d).

### Interaction of Breast Cancer Cells with the Extracellular Collagen Matrix

When cultured on collagen scaffolds, the two cell lines generated tissue-like structures and maintained their distinctive features: MCF-7 displayed an epithelial-like morphology with a tightly cohesive cobblestone appearance, while MDA-MB-231 showed a mesenchymal phenotype with lower cell-to-cell contact and a spindle appearance (Fig. 4a). Both cell lines proliferated within the scaffold, and on day 10 the number of cells reached about  $9 \times 10^6$  for MCF-7 and  $9.8 \times 10^6$  for MDA-MB-231 (Fig. 4b). Gene expression analysis showed that MCF-7 had a high level of E-cadherin expression but low vimentin, while MDA-MB-231 showed lower levels of E-cadherin and a high vimentin expression (Fig. 4c). MDA-MB-231 proved capable of internalizing collagen: confocal images of the scaffold matrix revealed the presence of blue collagen spots in the scaffolds cellularized with MDA-MB-231. These signals were not detectable in empty scaffolds or in the presence of MCF-7 cells (Fig. 4d). The collagen spots showed an intracellular localization that was further highlighted in images processed with ImageJ software (Fig. 4e).

### Assessment of the Prototype Loading Device Repeatability

Preliminary tests were performed on MDA-MB-231-cultured scaffolds to evaluate the repeatability of the measures obtained with the prototype loading device. The instrument and setting conditions exhibited good consistency that resulted in homogeneous dispersion of the different measures, as well as of the average values of technical replicates (Fig. 5a). The

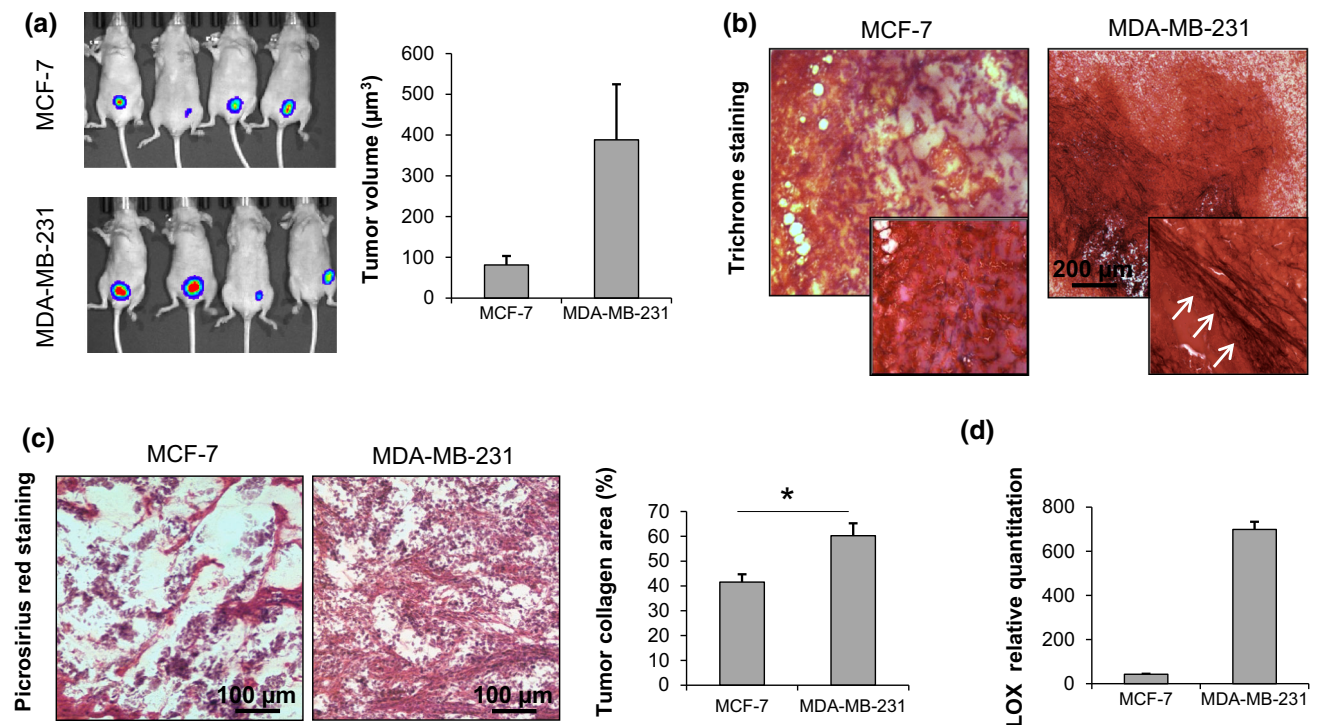


**FIGURE 3.** (a) Bioluminescence imaging of mammary tumors in nude mice generated by orthotopic injection of MCF-7 or MDA-MB-231 and caliper measurement of tumor volume after 4 weeks ( $\mu\text{m}^3$ ); (b) trichrome staining of OCT-embedded MCF-7 and MDA-MB-231 orthotopic tumors; (c) Picrosirius red staining of OCT-embedded MCF-7 and MDA-MB-231 orthotopic tumors with quantification of the mean percentage of collagen to total area; (d) relative quantitation values of LOX in MCF-7 and MDA-MB-231 orthotopic tumors. Data are mean  $\pm$  SE. \*  $p < 0.05$ .

intra-assay coefficient of variation was 10.7%, which was deemed sufficient for our purposes. No conditioning effect was detected when the same specimen was repeatedly loaded.

#### *Alteration of the Compressive Stiffness of Collagen Scaffolds by Invasive Breast Cancer Cells*

We investigated the effect of MCF-7 and MDA-MB-231 on the stiffness properties of collagen scaffolds by comparing the compressive modulus of uncellularized samples with that of samples decellularized after 10 days of culture with either cell line. The efficacy of the decellularization process was confirmed by MTT metabolization, which was virtually absent in decellularized samples (Fig. 5b). Furthermore, the DNA content decreased from  $175.9 \pm 16.46$  ng/ $\mu\text{L}$  for cellularized scaffolds to  $11.1 \pm 4.9$  ng/ $\mu\text{L}$  for decellularized scaffolds (Fig. 5c). MCF-7 did not significantly affect the mechanical properties of the scaffolds: uncellularized samples displayed an average compressive modulus of  $47.1 \pm 1.8$  kPa, while samples decellularized after MCF-7 culture showed an average compressive modulus of  $48.9 \pm 1.3$  kPa. Conversely, MDA-MB-231 cells produced a significant ( $p = 0.038$ ) increase in the scaffold stiffness: uncellularized samples

displayed an average compressive modulus of  $46.9 \pm 2.7$  kPa, while samples decellularized after MDA-MB-231 culture had an average compressive modulus of  $57.9 \pm 3.6$  kPa (Fig. 5d). Scaffold compressive modulus increased by 23% after MDA-MB-231 cell culture, in sharp contrast to the increase observed after culture with MCF-7 ( $< 5\%$ ) (Fig. 5e). Finally, MDA-MB-231 within the collagen scaffolds showed around a 1000-fold higher expression level of LOX than MCF-7 (Fig. 5f).

#### *Collagen Scaffold Remodeling by Breast Cancer Cells*

After 10 days' culture within the scaffold, MCF-7 and MDA-MB-231 cells altered the structural micro and macro characteristics of the collagen matrix. A significant decrease in the scaffold swelling property was produced by both cell lines with respect to uncellularized samples ( $p = 0.022$  for MCF-7 and  $p = 0.042$  for MDA-MB-231) (Fig. 6a). The average porosity was also reduced, albeit not significantly (Fig. 6b). Both cell lines decreased the mean pore area of the scaffold, but the decrease produced by MDA-MB-231 was markedly higher compared to that of MCF-7 ( $p = 0.002$  for MDA-MB-231) (Fig. 6c). SEM analysis showed the presence of a rough and irregular

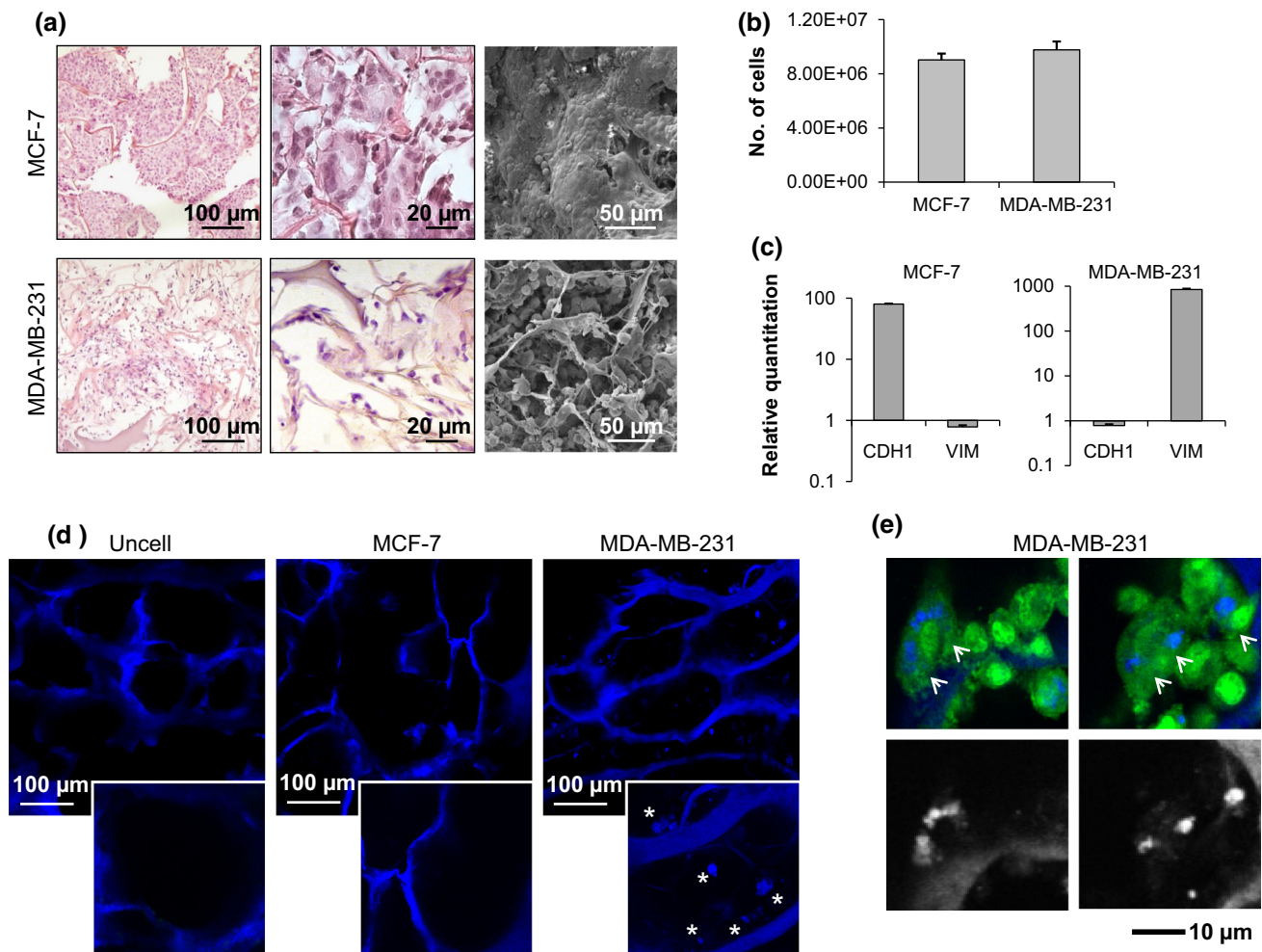


**FIGURE 4.** (a) Hematoxylin & eosin staining of paraffin-embedded sections of the 3D scaffolds cultured with MCF-7 or MDA-MB-231, and SEM imaging of scaffolds cultured with MCF-7 or MDA-MB-231; (b) number of MCF-7 and MDA-MB-231 infiltrating the scaffold on day 10; (c) relative quantitation values of E-cadherin (CDH1) and vimentin (VIM) in MCF-7 and MDA-MB-231 cells; (d) confocal images of the collagen matrix (blue, autofluorescence) of an empty scaffold (uncell) and of scaffolds cellularized with MCF-7 or MDA-MB-231; (e) confocal microscopy analysis of GFP-labeled MDA-MB-231 (green, GFP) on collagen scaffolds (blue, autofluorescence) and processed images to exclude the cell signal. Data are mean  $\pm$  standard error (SE).

matrix over the scaffold surface after MCF-7 and MDA-MB-231 culture, whereas uncellularized samples displayed a smooth and regular surface (Fig. 6d).

Collagen quantification by Picosirius red staining showed that the two cell lines did not increase the collagen content of the scaffold with respect to uncellularized samples (Fig. 6e). This result suggests that matrix proteins other than collagen were deposited by the two cell lines.

The scaffold matrix architecture differed markedly between uncellularized samples and samples cultured with MCF-7 or MDA-MB-231, as detected by Masson's trichrome staining. In particular, the matrix appeared more organized, densely packed and with linear collagen fibers (arrowhead) in the presence of MDA-MB-231, whereas uncellularized scaffolds and

scaffolds cultured with MCF-7 displayed a more dispersed and disorganized matrix (Fig. 7a).

#### *Impairment of MDA-MB-231 Cell Ability to Increase Collagen Stiffness by LOX Inhibition*

The survival percentage of BAPN-treated MDA-MB-231 cells was similar to that of untreated controls, indicating that BAPN did not affect proliferation (Fig. 7b). In the presence of LOX inhibition the ability of MDA-MB-231 cells to increase the stiffness of the collagen scaffold was reduced: uncellularized samples displayed an average compressive modulus of  $55.5 \pm 2.6$  kPa, while samples decellularized after MDA-MB-231 culture with BAPN treatment showed an average compressive modulus of  $58.1 \pm 5.2$  kPa

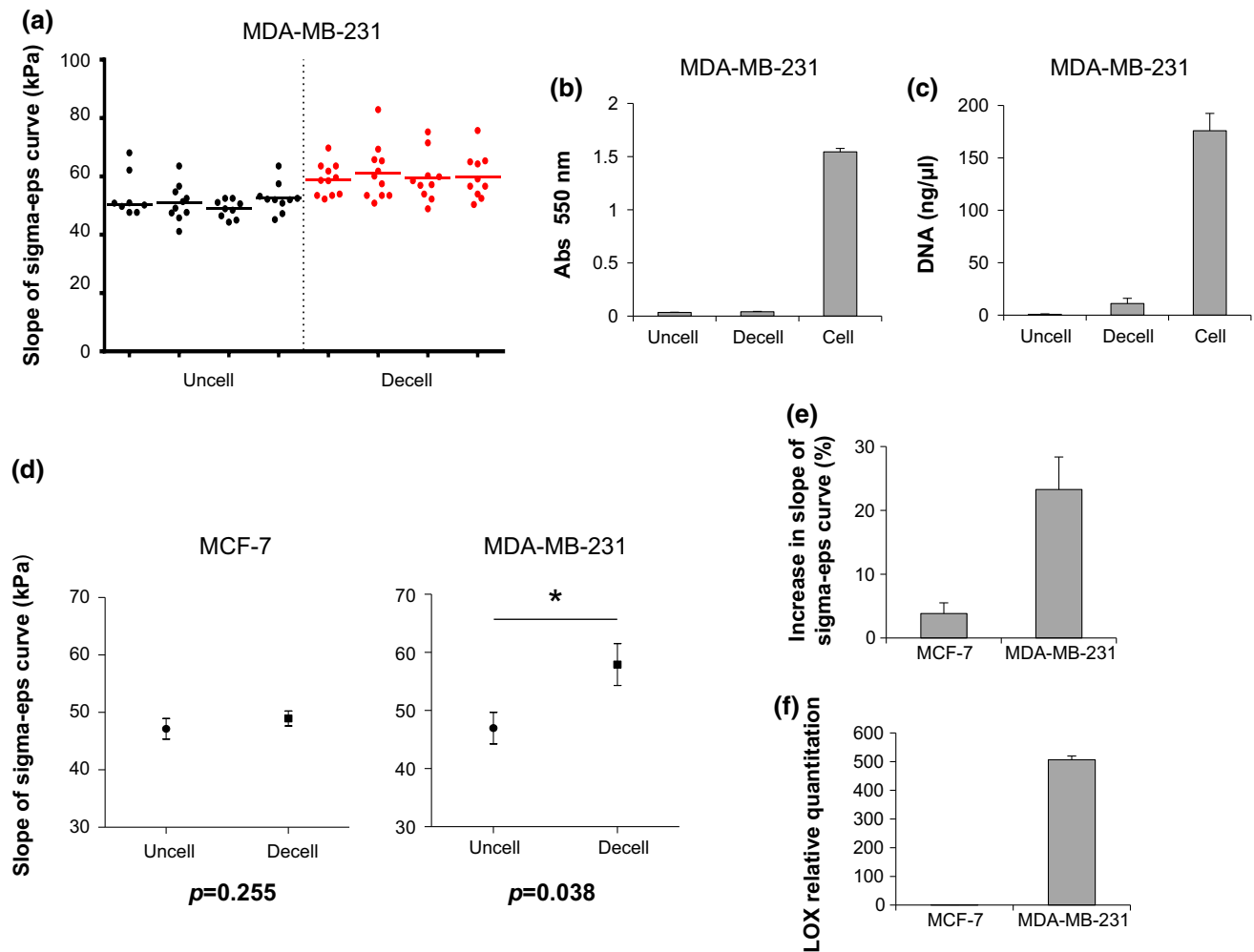


**FIGURE 5.** (a) Stiffness values for uncellularized (uncell) scaffolds or for scaffolds decellularized (decell) after a 10-day culture with MDA-MB-231, expressed as the slope of the sigma-epsilon curve (sigma-eps) (kPa); (b) 550 nm absorbance of uncellularized, cellularized (cell) or decellularized MTT-stained scaffolds; (c) DNA content (ng/ $\mu$ L) of uncellularized, cellularized or decellularized scaffolds or for scaffolds decellularized after a 10-day culture with MCF-7 or with MDA-MB-231; (d) average slope of the sigma-eps curve (kPa) for uncellularized scaffolds or for scaffolds decellularized after a 10-day culture with MCF-7 or with MDA-MB-231 with respect to uncellularized scaffolds; (e) percentage increase in the slope of the sigma-eps curve for scaffolds decellularized after a 10-day culture with MCF-7 or MDA-MB-231 with respect to uncellularized scaffolds; (f) relative quantitation values of LOX in MCF-7 and MDA-MB231. Data are mean  $\pm$  SE. \*  $p < 0.05$ .

(Fig. 7c). Scaffold compressive modulus increased by 8.9% with LOX inhibition compared to 23% without LOX inhibition (Fig. 7d).

## DISCUSSION

A dynamic mechanical interaction subsists between cancer cells and the surrounding ECM environment and governs essential tumor processes.<sup>23</sup> Thus, investigating the cancer mechanobiology represents a great opportunity to achieve a better understanding of the disease and to identify novel therapeutic targets or prognostic biomarkers. Three-dimensional scaffolds that enable the tuning of matrix microstructure, stiffness and composition offer a unique *in vitro* experi-

mental model to study the effects exerted by these biochemical and physical parameters on the behavior of cancer cells.<sup>20,24,36</sup> In this study we have utilized type I collagen scaffolds as an *in vitro* 3D biomimetic model to study the cell-ECM interaction occurring between either MDA-MB-231 or MCF-7 breast cancer cells, that are known to have different clinical aggressiveness.<sup>17</sup> Towards this end, our collagen scaffolds were the model of choice, as it (i) resembled the main component of the ECM; (ii) can be easily fabricated; (iii) and each feature can be tuned (e.g. structure, pore size, porosity, wettability, degradation).<sup>26</sup>

Mechanical signaling from the ECM influence different tumor phenotypes,<sup>29,37,38</sup> and the mechanical characteristics of tumors and tumor cells are predictive of the disease clinical behavior.<sup>31,41</sup> We first showed

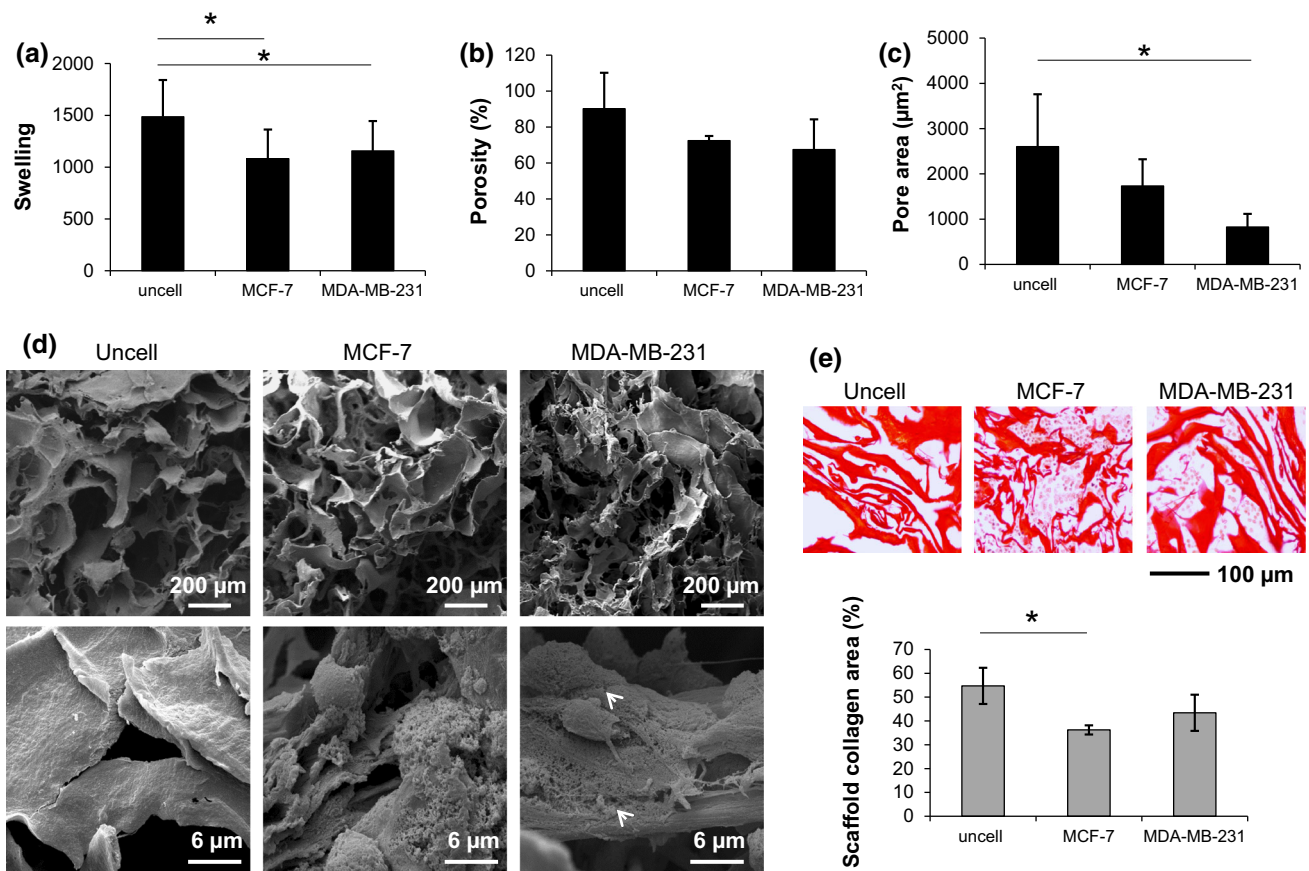


**FIGURE 6.** (a) Swelling property, (b) average porosity (%) and (c) average pore area of collagen scaffolds of samples without cells (uncell) and samples decellularized after a 10-day culture with MCF-7 or MDA-MB-231; (d) SEM analysis at different magnifications of the scaffolds without cells (uncell) and decellularized after a 10-day culture with MCF-7 or MDA-MB-231; (e) Picrosirius red staining of paraffin-embedded scaffolds without cells (uncell) and decellularized after a 10-day culture with MCF-7 or MDA-MB-231, with quantification of the mean percentage of collagen with respect to the total area. Data are mean  $\pm$  SE. \*  $p < 0.05$ . N.B. The decellularization process was also performed on empty scaffolds to avoid any bias between samples without cells and samples decellularized after culture with MCF-7 or MDA-MB-231; the decellularization process affected the scaffold structure, as shown by SEM analysis.

that *in vivo* orthotopic tumors generated by MDA-MB-231 cells, belonging to the more aggressive basal-like subtype, were characterized by elevated collagen content and high expression of LOX compared to tumors generated by MCF-7. Increased LOX levels and tumor stiffness have been associated with progression<sup>7,24,28,30</sup> and local invasion *via* oriented cell migration on aligned collagen fibers.<sup>32</sup> Moreover, the elevated expression of fibrillar collagens has been linked to the invasive and aggressive behavior of breast tumors.<sup>43</sup> Similar changes have been described by Acerbi and colleagues in specific subtypes of breast cancers. The authors found that the stroma at the invasive region of basal-like and Her-2 tumor subtypes was the most heterogeneous and the stiffest when compared to the less aggressive luminal A and B subtypes.<sup>1</sup> The two cell lines within the scaffolds preserved their specific phenotypes. Weakly aggressive MCF-7 cells displayed an epithelial-like morphology and a

high expression of the E-cadherin epithelial marker. Conversely, MDA-MB-231 showed an infiltrating and mesenchymal phenotype with lower E-cadherin expression and high levels of vimentin. Loss of E-cadherin is a key step in the epithelial to mesenchymal transition (EMT) process and has been implicated in cancer progression and metastasis, while vimentin expression drives a number of cellular processes including motility.<sup>25</sup> Using an originally-developed prototype instrument to assess the compression-dependent viscoelastic properties of collagen scaffolds, we were able to show that MDA-MB-231 produced a significant increase in macroscopic stiffness of our *in vitro* biomimetic model. While both cell lines induced a decrease in the scaffold swelling property and pore area, probably as a result of new matrix deposition, MDA-MB-231 cells proved capable of remodeling the scaffold architecture, producing a more organized and densely packed matrix. This cell line

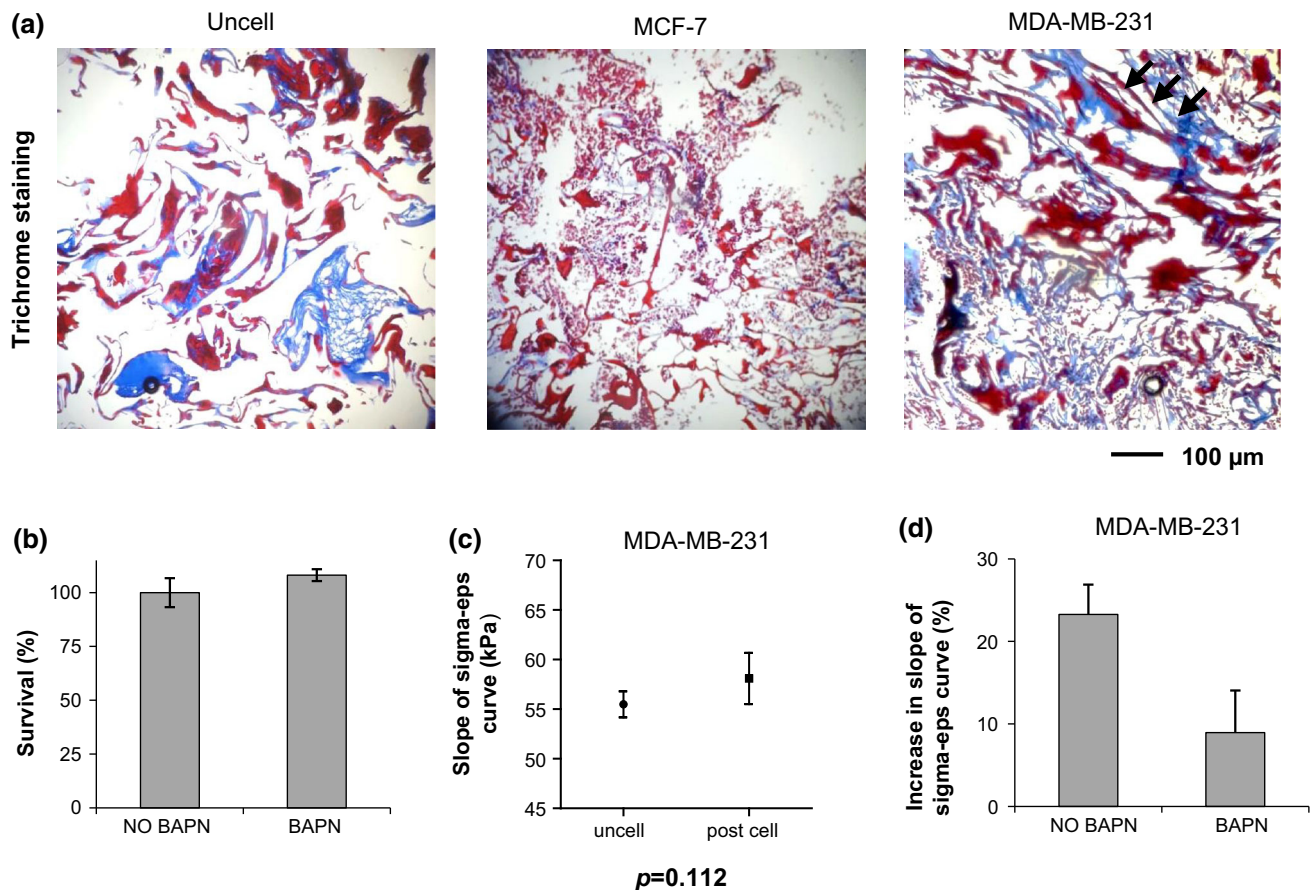


**FIGURE 7.** (a) Trichrome staining of paraffin-embedded scaffolds without cells (uncell) and decellularized after a 10-day culture with MCF-7 or MDA-MB-231; (b) Survival percentages of MDA-MB-231 cultured within the scaffold in the absence (NO BAPN) or presence (BAPN) of a LOX inhibitor; (c) average slope of the sigma-eps curve (kPa) for uncultured scaffolds or for scaffolds decellularized after a 10-day culture with MDA-MB-231 in the presence of LOX inhibition; (d) percentage increase in the slope of the sigma-eps curve for scaffolds decellularized after a 10-day culture with MDA-MB-231 in the presence or absence of LOX inhibition (BAPN and NO BAPN, respectively) with respect to uncellularized scaffolds. Data are mean  $\pm$  SE. \*  $p < 0.05$ .

expressed high levels of the collagen-crosslinking enzyme LOX both *in vivo* and in the collagen scaffolds. Conversely, MCF-7 expressed lower levels of LOX and did not significantly modify scaffold stiffness or architecture. Collagen crosslinking is related to its stiffness properties<sup>6</sup> and is, to a large extent, enzymatically catalyzed by the lysyl oxidase family.<sup>30</sup> When LOX activity was blocked, the ability of MDA-MB-231 to alter scaffold stiffness was impaired, providing a causal correlation between LOX-mediated collagen crosslinking and the observed increase in stiffness. Finally, MDA-MB-231 seemed to have the ability of collagen internalization which constitutes an important mechanism for ECM turnover and remodeling.<sup>10</sup> This process has been correlated with breast cancer progression and is mediated by the uPARAP/Endo180 receptor, expressed in basal-like breast tumor cells.<sup>39</sup> Recent findings have also shown that EMT is able to

enhance the ability of cancer cells to internalize collagen.<sup>18</sup>

Overall this work provides evidence that cancer cells belonging to the aggressive basal-like subtype of breast tumors display a greater ability to modify the surrounding ECM and in particular are able to alter the mechanical properties of extracellular collagen. Although our scaffold did not reproduce all the physiological characteristics of the breast ECM (i.e. it displayed a larger pore size), the cells showed a strong interaction with this matrix. Furthermore, the increase observed in the scaffold stiffness is consistent with the collagen characteristics in *in vivo* tumors and with previous findings on the ECM of basal-like breast cancers.<sup>1</sup>

These observations demonstrate that 3D collagen scaffolds might constitute a relevant and informative experimental model to address the mechanobiology of cell-ECM interaction. Moreover, due to the

abundance of functional groups, collagen can be functionalized with further components of the ECM<sup>37</sup> and the properties of the matrix tuned to achieve different mechanical characteristics in order to investigate their role in the tumor phenotypes and behavior.

### ACKNOWLEDGEMENTS

The authors wish to thank Marco Palanca for his contribution to designing and fine-tuning the compression device. They also thank Silvia Bellissimo for editorial assistance.

### CONFLICTS OF INTEREST

Chiara Liverani, Laura Mercatali, Luca Cristofolini, Emanuele Giordano, Silvia Minardi, Giovanna Della Porta, Alessandro De Vita, Giacomo Miserochi, Chiara Spadazzi, Ennio Tasciotti, Dino Amadori and Toni Ibrahim have no conflicts of interest to declare.

### RESEARCH INVOLVING ANIMALS

All experimental animal procedures were reviewed and approved by the Institutional Animal Care and Use Committee (IACUC) of the Houston Methodist Research Institute (HMRI) protocol number AUP 0614-0033.

### REFERENCES

- <sup>1</sup>Acerbi, I., L. Cassereau, I. Dean, Q. Shi, A. Au, C. Park, Y. Y. Chen, J. Liphardt, E. S. Hwang, and V. M. Weaver. Human breast cancer invasion and aggression correlates with ECM stiffening and immune cell infiltration. *Integr. Biol. (Camb.)* 7:1120–1134, 2015.
- <sup>2</sup>Beer, F., E. Russell Johnson Jr., J. T. DeWolf, and D. F. Mazurek. *Mechanics of Materials* (6th ed.). New York: McGraw-Hill Publ., 2011.
- <sup>3</sup>Bergamaschi, A., E. Tagliabue, T. Sørli, B. Naume, T. Triulzi, R. Orlandi, H. G. Russnes, J. M. Nesland, R. Tammi, P. Auvinen, V. M. Kosma, S. Ménard, and A. L. Børresen-Dale. Extracellular matrix signature identifies breast cancer subgroups with different clinical outcome. *J. Pathol.* 214:357–367, 2008.
- <sup>4</sup>Bondareva, A., C. M. Downey, F. Ayres, W. Liu, S. K. Boyd, B. Hallgrímsson, and F. R. Jirik. The lysyl oxidase inhibitor,  $\beta$ -aminopropionitrile, diminishes the metastatic colonization potential of circulating breast cancer cells. *PLoS ONE* 4:e5620, 2009.
- <sup>5</sup>Bonnans, C., J. Chou, and Z. Werb. Remodelling the extracellular matrix in development and disease. *Nat. Rev. Mol. Cell Biol.* 15:786–801, 2014.

- <sup>6</sup>Buehler, M. J. Nature designs tough collagen: explaining the nanostructure of collagen fibrils. *Proc. Natl. Acad. Sci. USA* 103:12285–12290, 2006.
- <sup>7</sup>Butcher, D. T., T. Alliston, and V. M. Weaver. A tense situation: forcing tumour progression. *Nat. Rev. Cancer* 9:108–122, 2009.
- <sup>8</sup>Carey, S. P., T. M. D’Alfonso, S. J. Shin, and C. A. Reinhart-King. Mechanobiology of tumor invasion: engineering meets oncology. *Crit. Rev. Oncol. Hematol.* 83:170–183, 2012.
- <sup>9</sup>Cassereau, L., Y. A. Miroshnikova, G. Ou, J. Lakins, and V. M. Weaver. A 3D tension bioreactor platform to study the interplay between ECM stiffness and tumor phenotype. *J. Biotechnol.* 193:66–69, 2015.
- <sup>10</sup>Curino, A. C., L. H. Engelholm, S. S. Yamada, K. Holmbeck, L. R. Lund, A. A. Molinolo, N. Behrendt, B. S. Nielsen, and T. H. Bugge. Intracellular collagen degradation mediated by uPARAP/Endo180 is a major pathway of extracellular matrix turnover during malignancy. *J. Cell Biol.* 169:977–985, 2005.
- <sup>11</sup>Cuzick, J., J. Warwick, E. Pinney, S. W. Duffy, S. Cawthorn, A. Howell, J. F. Forbes, and R. M. Warren. Tamoxifen-induced reduction in mammographic density and breast cancer risk reduction: a nested case–control study. *J. Natl. Cancer Inst.* 103:744–752, 2011.
- <sup>12</sup>Du Fort, C. C., M. J. Paszek, and V. M. Weaver. Balancing forces: architectural control of mechanotransduction. *Nat. Rev. Mol. Cell Biol.* 12:308–319, 2011.
- <sup>13</sup>Dvorak, H. F., V. M. Weaver, T. D. Tlsty, and G. Bergers. Tumor microenvironment and progression. *J. Surg. Oncol.* 103:468–474, 2011.
- <sup>14</sup>Elsamany, S., A. Alzahrani, S. A. Elkhaliq, O. Elemam, E. Rawah, M. U. Farooq, M. Almatrafi, and F. K. Olayan. Prognostic value of mammographic breast density in patients with metastatic breast cancer. *Med. Oncol.* 31:96, 2014.
- <sup>15</sup>Engler, A. J., S. Sen, H. L. Sweeney, and D. E. Discher. Matrix elasticity directs stem cell lineage specification. *Cell* 126:677–689, 2006.
- <sup>16</sup>Fenner, J., A. C. Stacer, F. Winterroth, T. D. Johnson, K. E. Luker, and G. D. Luker. Macroscopic stiffness of breast tumors predicts metastasis. *Sci. Rep.* 4:5512, 2014.
- <sup>17</sup>Holliday, D. L., and V. Speirs. Choosing the right cell line for breast cancer research. *Breast Cancer Res.* 13:215, 2011.
- <sup>18</sup>Huijbers, I. J., M. Iravani, S. Popov, D. Robertson, S. Al-Sarraj, C. Jones, and C. M. Isacke. A role for fibrillar collagen deposition and the collagen internalization receptor endo180 in glioma invasion. *PLoS ONE* 5:e9808, 2010.
- <sup>19</sup>Infanger, D. W., M. E. Lynch, and C. Fischbach. Engineered culture models for studies of tumor–microenvironment interactions. *Annu. Rev. Biomed. Eng.* 15:29–53, 2013.
- <sup>20</sup>Insua-Rodríguez, J., and T. Oskarsson. The extracellular matrix in breast cancer. *Adv. Drug Deliv. Rev.* 97:41–55, 2016.
- <sup>21</sup>Janmey, P. A., and R. T. Miller. Mechanisms of mechanical signaling in development and disease. *J. Cell Sci.* 124:9–18, 2011.
- <sup>22</sup>Kang, Y., P. M. Siegel, W. Shu, M. Drobnjak, S. M. Kakonen, C. Córdón-Cardo, T. A. Guise, and J. Masagué. A multigenic program mediating breast cancer metastasis to bone. *Cancer Cell* 3:537–549, 2003.
- <sup>23</sup>Kumar, S., and V. M. Weaver. Mechanics, malignancy, and metastasis: the force journey of a tumor cell. *Cancer Metastasis Rev.* 28:113–127, 2009.

- <sup>24</sup>Levental, K. R., H. Yu, L. Kass, J. N. Lakins, M. Egeblad, J. T. Erler, S. F. Fong, K. Csiszar, A. Giaccia, W. Weninger, M. Yamauchi, D. L. Gasser, and V. M. Weaver. Matrix crosslinking forces tumor progression by enhancing integrin signaling. *Cell* 139:891–906, 2009.
- <sup>25</sup>Mendez, M. G., S. Kojima, and R. D. Goldman. Vimentin induces changes in cell shape, motility, and adhesion during the epithelial to mesenchymal transition. *FASEB J.* 24:1838–1851, 2010.
- <sup>26</sup>Minardi, S., M. Sandri, J. O. Martinez, I. K. Yazdi, X. Liu, M. Ferrari, B. K. Weiner, A. Tampieri, and E. Tasciotti. Multiscale patterning of a biomimetic scaffold integrated with composite microspheres. *Small* 10:3943–3953, 2014.
- <sup>27</sup>Nilsson, M., H. Adamo, A. Bergh, and S. HalinBergström. Inhibition of lysyl oxidase and lysyl oxidase-like enzymes has tumour-promoting and tumour-suppressing roles in experimental prostate cancer. *Sci. Rep.* 6:19, 2016.
- <sup>28</sup>Oskarsson, T. Extracellular matrix components in breast cancer progression and metastasis. *Breast* 22(Suppl. 2):S66–S72, 2013.
- <sup>29</sup>Paszek, M. J., N. Zahir, K. R. Johnson, J. N. Lakins, G. I. Rozenberg, A. Gefen, C. A. Reinhart-King, S. S. Margulies, M. Dembo, D. Boettiger, D. A. Hammer, and V. M. Weaver. Tensional homeostasis and the malignant phenotype. *Cancer Cell* 8:241–254, 2005.
- <sup>30</sup>Payne, S. L., M. J. Hendrix, and D. A. Kirschmann. Paradoxical roles for lysyl oxidases in cancer—a prospect. *J. Cell. Biochem.* 101:1338–1354, 2007.
- <sup>31</sup>Plodinec, M., M. Loparic, C. A. Monnier, E. C. Obermann, R. Zanetti-Dallenbach, P. Oertle, J. T. Hyotyla, U. Aebi, M. Bentires-Alj, R. Y. Lim, and C. A. Schoenberger. The nanomechanical signature of breast cancer. *Nat. Nanotechnol.* 7:757–765, 2012.
- <sup>32</sup>Provenzano, P. P., K. W. Eliceiri, J. M. Campbell, D. R. Inman, J. G. White, and P. J. Keely. Collagen reorganization at the tumor-stromal interface facilitates local invasion. *BMC Med.* 4:38, 2006.
- <sup>33</sup>Psaila, B., and D. Lyden. The metastatic niche: adapting the foreign soil. *Nat. Rev Cancer* 9:285–293, 2009.
- <sup>34</sup>Roeder, B. A., K. Kokini, J. E. Sturgis, J. P. Robinson, and S. L. Voytik-Harbin. Tensile mechanical properties of three-dimensional type I collagen extracellular matrices with varied microstructure. *J. Biomech. Eng.* 124:214–222, 2002.
- <sup>35</sup>Schedin, P., and J. P. Keely. Mammary gland ECM remodeling, stiffness, and mechanosignaling in normal development and tumor progression. *Cold Spring Harb. Perspect. Biol.* 3:a003228, 2011.
- <sup>36</sup>Shawn, P. C., C. M. Kraning-Rush, R. M. Williams, and C. A. Reinhart-King. Biophysical control of invasive tumor cell behavior by extracellular matrix microarchitecture. *Biomaterials* 33:4157–4165, 2012.
- <sup>37</sup>Tan, Y., A. Tajik, J. Chen, Q. Jia, F. Chowdhury, L. Wang, J. Chen, S. Zhang, Y. Hong, H. Yi, D. C. Wu, Y. Zhang, F. Wei, Y. C. Poh, J. Seong, R. Singh, L. J. Lin, S. Doğanay, Y. Li, H. Jia, T. Ha, Y. Wang, B. Huang, and N. Wang. Matrix softness regulates plasticity of tumour-repopulating cells via H3K9 demethylation and Sox2 expression. *Nat. Commun.* 5:4619, 2014.
- <sup>38</sup>Ulrich, T. A., E. M. de Juan Pardo, and S. Kumar. The mechanical rigidity of the extracellular matrix regulates the structure, motility, and proliferation of glioma cells. *Cancer Res.* 69:4167–4174, 2009.
- <sup>39</sup>Wienke, D., G. C. Davies, D. A. Johnson, J. Sturge, M. B. Lambros, K. Savage, S. E. Elsheikh, A. R. Green, I. O. Ellis, D. Robertson, J. S. Reis-Filho, and C. M. Isacke. The collagen receptor Endo180 (CD280) is expressed on basal-like breast tumor cells and promotes tumor growth in vivo. *Cancer Res.* 67:10230–10240, 2007.
- <sup>40</sup>Wozniak, M. A., and P. J. Keely. Use of three-dimensional collagen gels to study mechanotransduction in T47D breast epithelial cells. *Biol. Proced. Online* 7:144–161, 2005.
- <sup>41</sup>Xu, W., R. Mezenzev, B. Kim, L. Wang, J. McDonald, and T. Sulchek. Cell stiffness is a biomarker of the metastatic potential of ovarian cancer cells. *PLoS ONE* 7:e46609, 2012.
- <sup>42</sup>Yang, X., S. Li, W. Li, J. Chen, X. Xiao, Y. Wang, G. Yan, and L. Chen. Inactivation of lysyl oxidase by  $\beta$ -aminopropionitrile inhibits hypoxia-induced invasion and migration of cervical cancer cells. *Oncol. Rep.* 29:541–548, 2013.
- <sup>43</sup>Zaman, M. H., L. M. Trapani, A. L. Sieminski, D. Mackellar, H. Gong, R. D. Kamm, A. Wells, D. A. Lauffenburger, and P. Matsudaira. Migration of tumor cells in 3D matrices is governed by matrix stiffness along with cell-matrix adhesion and proteolysis. *Proc. Natl. Acad. Sci. USA* 103:10889–10894, 2006.